Frontiers in Bioscience Landmark

Front. Biosci. (Landmark Ed) **2025**; 30(5): 36430
https://doi.org/10.31083/FBL36430

Original Research

Inhibition of Phosphoglycerate Kinase 1 Enhances Radiosensitivity of Esophageal Squamous Cell Carcinoma to X-rays and Carbon Ion Irradiation

Junru Chen[1,2,†], Hongtao Luo[1,†], Xun Wu[1,2], Meng Dong[1,2], Dandan Wang[1,2], Yuhong Ou[1,2], Yuhang Wang[1,2], Shilong Sun[1], Zhiqiang Liu[1], Zhen Yang[3], Quanlin Guan[2], Qiuning Zhang[1,*]

[1]Institute of Modern Physics, Chinese Academy of Sciences, 730000 Lanzhou, Gansu, China
[2]The First School of Clinical Medicine, Lanzhou University, 730000 Lanzhou, Gansu, China
[3]School of Public Health, Gansu University of Chinese Medicine, 730030 Lanzhou, Gansu, China
*Correspondence: 523249930@qq.com (Qiuning Zhang)
[†]These authors contributed equally.

Academic Editors: Alexandros G. Georgakilas and Milena Georgieva
Submitted: 18 December 2024 Revised: 27 March 2025 Accepted: 24 April 2025 Published: 23 May 2025

Abstract

Background: Radiotherapy is crucial for managing esophageal squamous cell carcinoma (ESCC). This research explored the potential and mechanism of enhancing ESCC radiosensitivity through targeting phosphoglycerate kinase 1 (PGK1). **Methods**: After ESCC cells were exposed to X-rays and C-ions, hub genes were identified through proteomic analysis and bioinformatics. To elucidate PGK1's function, small interfering RNAs and plasmids were used to silence and overexpress PGK1 in two human ESCC cell lines. Plate colony formation, cell counting kit 8, and 5-ethynyl-2′-deoxyuridine assays were conducted to detect cell proliferation after irradiation with different linear energy transfer rays (X-rays and carbon ions). Flow cytometry was used to assess radiation-induced perturbations in the cell cycle, apoptosis, reactive oxygen species (ROS), and mitochondrial membrane potential. Western blotting was performed to detect the protein expressions of protein kinase B (Akt), phosphorylated protein Kinase B (pAkt), mammalian target of rapamycin (mTOR), and phosphorylated mammalian target of rapamycin (pmTOR). **Results**: Proteomics and bioinformatics analyses revealed that PGK1 plays a key role in modulating ESCC radiosensitivity. Knockdown of PGK1 resulted in the suppression of cancer cell proliferation and viability, promoted apoptotic processes, and demonstrated a synergistic anti-tumor effect in conjunction with radiation. Conversely, overexpression of PGK1 promoted cancer cell growth and increased radiation resistance. This may be attributed to the accumulation of ROS and the inhibition of Akt/mTOR pathway following PGK1 inhibition. **Conclusion**: Targeting PGK1 may be an effective strategy to increase ESCC radiation sensitivity, offering a promising strategy for improving treatment outcomes.

Keywords: ionizing radiation; phosphoglycerate kinase 1; reactive oxygen species; radiosensitivity; carbon ions

1. Introduction

Esophageal carcinoma (ESCA) is a prevalent neoplastic disease of the gastrointestinal tract in China, representing over 40% of global cases [1]. Esophageal squamous cell carcinoma (ESCC) is the most prevalent histological subtype worldwide, comprising more than 85% of ESCA cases in China [2,3]. Ionizing radiation (IR) serves as a primary therapeutic modality for ESCC, particularly in patients deemed inoperable. However, the local control rates and survival outcomes for patients with inoperable ESCA remain concerning, even with the implementation of up to 60 Gy of definitive radiotherapy, with local recurrence occurring in 40%–60% of patients [3,4]. A study has shown that increasing radiation doses for esophageal cancer does not lead to better survival but rather increases radiation-induced damage [5]. Therefore, effectively improving the radiosensitivity and reducing metastasis and recurrence following ESCC radiotherapy represent significant challenges for ESCC radiotherapy.

Phosphoglycerate kinase 1 (PGK1) serves as the initial enzyme to produce ATP within the glycolytic. It catalyzes the ADP phosphorylation by transferring a phosphate group from 1,3-bisphosphoglycerate, resulting in the formation of 3-phosphoglycerate and ATP reversibly. PGK1 is notably elevated in cancers such as ESCA, cervical carcinoma, and lung squamous cell carcinoma, showing a significant correlation with the survival and prognosis [6]. Functioning as both a glycolytic enzyme and protein kinase, PGK1 modulates cellular metabolism by coordinating glycolysis with the mitochondrial tricarboxylic acid cycle [7]. Moreover, PGK1 participates in angiogenesis, DNA replication and repair, and autophagy initiation, and it is essential for tumorigenesis and development [7,8]. Nevertheless, the function of PGK1 in the context of IR in tumor cells remains largely unexplored.

Currently, radiotherapy for esophageal cancer mainly utilizes X-rays. However, clinical evidence from multiple cancer centers indicates that carbon ion radiother-

apy (CIRT) is also an effective and feasible option for esophageal cancer [9,10]. Compared with photons (X-rays), C-ions exhibit a higher linear energy transfer (LET), resulting in more significant biological damage. Moreover, C-ions release an enormous amount of energy at the end of their range, offering advantages for both tumor treatment and sparing of surrounding healthy tissues. As radiotherapy technology progresses and clinical trials deepen, C-ions radiotherapy may become an increasingly important treatment modality for esophageal cancer patients.

In this study, we analyzed the mass spectrometry results of ECA-109 cells after X-rays and C-ions irradiation, and found that PGK1 is a key molecule involved in the radiation response. Subsequently, we investigated the function of PGK1 during X-rays and C-ions irradiation of ESCC cells regarding proliferation, apoptosis, and the cell cycle. Our results suggest that highly expressed PGK1 inhibits the radiosensitivity of ESCC, which may be linked to reducing reactive oxygen species (ROS)-mediated mitochondrial damage and the activation of the protein kinase B (Akt)/mammalian target of rapamycin (mTOR) signaling pathway. This study not only revealed the function of PGK1 during ionizing radiation in ESCC cells but also provided insights into its signal transduction mechanism. These findings deepen our comprehension of IR resistance and present a reasonable therapeutic target to augment the radiosensitivity of ESCC cells.

2. Materials and Methods

2.1 Cell Culture

The human ESCC cell lines, ECA-109 and KYSE-150, were purchased from Sun Yat-sen Memorial Hospital (Guangzhou, China). Additionally, the human normal esophageal cell line, HEEC, was obtained from the BeNa Culture Collection (BNCC359279, BNCC, Beijing, China). These cells were maintained under RIPM-1640 medium (SH30809.01, Hyclone, Logan, UT, USA) supplemented with 10% fetal bovine serum (FBS) (FSP500, ExCell Bio, Shanghai, China), 100× penicillin-streptomycin liquid (P1400, Solarbio, Beijing, China). Cultivation was carried out at 37 °C with 5% CO_2 atmosphere. All cell lines were validated by STR profiling tested for Mycoplasma contamination by MycoStripe (rep-mys-10, InvivoGen, San Diego, CA, USA).

2.2 TMT Quantitative Proteomic

For proteomic investigation, ECA109 cellular samples were harvested following a 48-hour incubation period post-irradiation, including three treatment conditions: non-irradiated controls (0 Gy), X-ray exposure at 2 Gy, and C-ions irradiation at 2 Gy. Specific experimental procedures were performed as previously described [11]. Following data acquisition, MS/MS results were processed through the Proteome Discoverer 2.2 platform (Waltham, MA, USA), employing the Matrix Science's Search and Correlation Tool (MASCOT) algorithm 2.6 (Matrix Science, London, UK) for protein identification against the UniProt (http://www.uniprot.org) reference database. Proteins were deemed significantly altered if they met both criteria: fold change $\geq$1.2 and $p < 0.05$.

2.3 Bioinformatics Analysis

To assess variability within and between groups, Principal Component Analysis (PCA) was conducted on all reliably identified proteins using the factoextra package in R software 4.3.2 (CRAN, Vienna, Austria). The overlapping patterns of differentially expressed proteins (DEPs) were visualized via EVenn (http://www.ehbio.com/test/venn/#/). Heatmaps of overlapping DEPs were generated using the "heatmap" package of R software. Enrichment analyses for Gene Ontology (GO) and the Kyoto Encyclopedia of Genes and Genomes (KEGG) were conducted using R's "clusterProfile" package. The STRING database (https://string-db.org/) was employed to generate protein-protein interaction (PPI) networks. Then, PPI networks were analyzed in Cytoscape 3.9.1 (Cytoscape Consortium, San Diego, CA, USA) via cytoHubba, and top five hub proteins were identified based on centrality. Consensus hub proteins derived from 12 independent algorithms were determined by Venn analysis (http://www.ehbio.com/test/venn/#/). Esophageal cancer data from The Cancer Genome Atlas (TCGA) and Genotype-Tissue Expression (GTEx) were obtained via UCSC Xena (https://xenabrowser.net). Survival analysis used R's maxstat for optimal mRNA cut-off determination, with ggplot2 for boxplots and Kaplan-Meier curves.

2.4 Irradiation Conditions and Reagents

Radiation treatments were conducted using two modalities: C-ions irradiation (100 MeV/u, LET 50 keV/μm) with a 5 mm spread-out Bragg peak was delivered at Heavy Ion Research Facility in Lanzhou (Institute of Modern Physics, CAS, Lanzhou, Gansu, China) using a 10 × 10 cm field at 1 Gy/min; X-rays exposure (225 kV/13.3 mA) was performed using an X-Rad 225 system (Precision, North Branford, CT, USA) at identical dose rate.

N-acetyl-L-cysteine (NAC) (C8460, Solarbio, Beijing, China) was dissolved in sterilized water and used in a final concentration of 10 mM in medium, which was administered 2 h prior to irradiation. Carbonyl cyanide m-chlorophenylhydrazone (CCCP) (C2008S-3, Beyotime, Shanghai, China) was used in a final concentration of 10 μM in medium.

2.5 RNA Interference and Overexpression Plasmid Transfection

GenePharma Co., Ltd. (Shanghai, China) commercially synthesized the small interfering RNA (siRNA) for PGK1 downregulation, the negative control (NC) siRNA, and the PGK1 overexpression plasmids. Following the manufacturer's guidelines to knockdown and overexpress PGK1 in cells. **Supplementary Table 1** lists the siRNA se-

quences used for gene silencing. The plasmid sequence utilized for PGK1 overexpression is detailed in **Supplementary Table 2**.

2.6 RNA Extraction and qRT-PCR

RNA was isolated with TRIzol (15596026CN, Invitrogen, Carlsbad, CA, USA) and reverse transcribed using a cDNA reverse transcription kit (11141ES10, Yeason, Shanghai, China) per manufacturer's protocol. qPCR was performed with a SYBR Green kit (11201ES08, Yeason, Shanghai, China) on a real-time PCR Detection System (ASA-4800, Baiyuan, Suzhou, Jiangsu, China). β-actin served as the internal reference for normalization. Gene expression was quantified via the $2^{-\Delta\Delta Ct}$ method. Primer sequences are provided in **Supplementary Table 3**.

2.7 Western Blot

Cellular proteins were lysed in RIPA buffer (R0010, Solarbio, Beijing, China) supplemented with protease inhibitors (P6730, Solarbio, Beijing, China) and phosphatase inhibitors (P1260, Solarbio, Beijing, China). Protein quantification was performed using a BCA assay kit (PC0020, Solarbio, Beijing, China). Samples were separated by 8%–12% SDS-PAGE and transferred to PVDF membranes (IPVH00010, Millipore, Burlington, MA, USA). After blocking with 5% skimmed milk or BSA, membranes were incubated with primary antibodies (overnight, 4 °C). Subsequently, 1.5 h incubation with HRP-conjugated secondary antibodies. Signal detection was achieved using enhanced chemiluminescence reagent (PE0010, Solarbio, Beijing, China) and visualized with a chemiluminescence detection system (GD50202, Monad, Zhejiang, Jiangsu, China). ImageJ software 1.54f (NIH, Bethesda, MD, USA) was then used to quantify the images. Antibody details are provided in **Supplementary Table 4**.

2.8 Clonogenic Formation Assay

Cells (300–6000 cells) were plated in Φ 60-mm dishes and cultured (37 °C, 5% CO_2) for 10–14 days. After formaldehyde fixation and 1.0% crystal violet (G1063, Solarbio, Beijing, China) staining, colonies (>50 cells) were counted by ImageJ software 1.54f. Clonogenic surviving fractions were calculated as (colonies counted/seeded cells) $\times$ 100, and normalized to non-irradiated controls. Survival curves were generated using the linear quadratic model (SF = e^(-(αD+βd^2))) in GraphPad Prism 9.0 (GraphPad Corp., San Diego, CA, USA). Relative biological effectiveness (RBE) values were determined as the ratio of X-rays to C-ions doses required for 10% survival.

2.9 Cell Proliferation Assay

2000 cells/well were seeded in a 96-well plate. 10 µL cell counting kit-8 (CCK-8) reagents (40203ES, Yeason, Shanghai, China) were introduced into each well, and the plate was subsequently maintained for 2 h. For 3 consecutive days, the absorbance at 450 nm was recorded using a microplate reader (Infinite M200 Pro, Tecan, Mannedorf, Zurich, Switzerland).

The 5-Ethynyl-2′-deoxyuridine (EdU) detection was performed using the Cell-Light™ EdU Apollo Kit per manufacturer's instructions (C10310-1, RIBOBIO, Guangzhou, Guangdong, China). Cells in 12-well plates were labeled with EdU for 2 h, and then stained in the dark for 30 min. Subsequently, nuclei were re-stained with Hoechst 33,342 for 30 min in the dark. Images were acquired by fluorescence microscopy (DP74, Olympus, Shinjuku, Tokyo, Japan).

2.10 Flow Cytometry

The Annexin V-FITC/PI apoptosis detection kit (MA0220, MeilunBio, Dalian, Liaoning, China) was used to evaluate apoptosis. Briefly, the harvested cell were treated with annexin V-FITC and PI in 1$\times$ binding buffer (15 min, dark). Cell cycle analysis required 75% ice-cold ethanol fixation and storage at –20 °C $\geq$ 2 h. Prior to analysis, fixed cells were centrifuged and washed according to the protocol of the Cell Cycle Staining Kit (CCS012, MULTI SCIENCES, Hangzhou, Zhejiang, China). Then, cells were stained with DNA staining solution in darkness for 30 min. Intracellular ROS was measured by the fluorescent probe DCFH-DA (S0033S, Beyotime, Shanghai, China), which was diluted in serum-free medium and used to incubate cells for 30 min at 37 °C. Mitochondrial membrane potential (MMP) was evaluated using Rhodamine 123 staining (C2008S, Beyotime, Shanghai, China). Cells were incubated in a serum-free medium containing the dye solution for 30 min under dark conditions. The staining results were measured by a flow cytometer (Model 100370, Amnis/Merck Millipore, Seattle, WA, USA). Data were analyzed using IDEAS 6.0 (Amnis/Merck Millipore, Seattle, WA, USA) or FlowJo 7.6 (Tree Star Inc., Ashland, OR, USA).

2.11 Statistical Analysis

We utilized GraphPad Prism 9.0 for both statistical computations and visualizations. For direct comparisons between just two groups, we relied on an unpaired *t*-test. However, for situations requiring analysis across several groups, we turned to one-way or two-way analysis of variance, complemented by post-hoc Bonferroni test. The log-rank test was employed for survival analysis. The statistical comparisons were all two-tailed, with *p*-values below 0.05 indicating statistical significance. Experimental data, derived from at least three independent replicates, are presented as means $\pm$ standard deviation.

3. Results

3.1 Screening of Key Proteins

First, we evaluated the consistency of the sample. The PCA results showed high aggregation among repeated samples and significant differences among different samples,

indicating good quantitative repeatability of the samples (Fig. 1A). A total of 521 DEPs were detected in the 2 Gy C-ions group compared to the control group, 412 DEPs between the 2 Gy C-ions and 2 Gy X-rays groups, and 352 DEPs between the 2 Gy X-rays group and the control group. The Venn diagram shows 33 overlapping DEPs in the three groups (Fig. 1B). The protein expression heatmap shows the expression levels of overlapping DEPs in different groups and samples (Fig. 1C). We conducted GO and KEGG enrichment analyses on these 33 DEPs to determine their functional characteristics. The findings from the GO enrichment analysis indicated that merely four terms exhibited significant enrichment within the molecular function (MF) category, predominantly related to disulfide oxidoreductase activity, oxidoreductase activity, and protein-disulfide reductase activity. The biological process and cellular components were not significantly enriched (Fig. 1E). KEGG enrichment analysis suggested that 33 DEPS were predominantly associated with carbon metabolism and the pentose phosphate pathway (Fig. 1E). To screen for hub proteins, a PPI network of the DEPs was constructed, with 11 nodes and 10 edges (Fig. 1F). The top five hub proteins were identified using twelve algorithms of the cytoHubba plug-in (**Supplementary Table 5**). Through the Venn diagram overlap of the hub proteins derived from the twelve algorithms, we identified three shared hub proteins, namely, PGK1, thioredoxin (TXN), and glucose-6-phosphate dehydrogenase (G6PD) (Fig. 1D).

Subsequently, we examined the mRNA levels of *PGK1*, *TXN*, and *G6PD* in normal esophageal tissues and esophageal tumor tissues. As displayed in Fig. 2D–F, the tumor cohort exhibited notably higher mRNA levels for *TXN*, *G6PD*, and *PGK1* compared to the normal group ($p < 0.001$), and their expression levels were greater in ESCC compared to EAC. We further evaluated the prognostic effect of *TXN*, *G6PD*, and *PGK1* mRNA expression levels in ESCA patients. The analysis revealed no significant association between *TXN* levels and overall survival (OS) in ESCA patients, including both esophageal adenocarcinoma (EAC) and ESCC ($p > 0.05$) (Fig. 2A). Elevated *G6PD* expression associated with unfavorable prognosis in ESCC patients ($p < 0.05$), while showing no significant impact on EAC ($p > 0.05$) (Fig. 2B). In both ESCC and EAC, high *PGK1* expression significantly reduced OS in these patients ($p < 0.05$) (Fig. 2C). Consequently, PGK1 was selected as the key molecule for subsequent experiments.

3.2 PGK1 Impacts the Regulation of IR Concerning the ESCC Cells Proliferation

Next, we found that the mRNA and protein levels of PGK1 was significantly higher in ESCC cell lines (ECA-109 and KYSE-150) compared to normal esophageal normal cell (HEEC) ($p < 0.01$). Specifically, the expression of *PGK1* mRNA and PGK1 protein (**Supplementary Fig. 1A**) and protein (Fig. 3A) was greater in ECA-109 cells compared to KYSE-150 cells ($p < 0.01$). We carried out Western Blotting experiments to explore the effects of radiation type and dose on PGK1 levels. The findings indicated that after lower doses of X-rays radiation, the PGK1 expression levels of ECA-109 and KYSE-150 cells increased significantly ($p < 0.05$), while they decreased significantly after higher doses radiation ($p < 0.05$). For C-ions, PGK1 expression in ECA-109 cells increased significantly after lower doses radiation and decreased significantly after higher doses radiation ($p < 0.05$); however, unlike ECA-109 cells, PGK1 expression in KYSE-150 cells did not increase significantly after lower doses of C-ions radiation. Although PGK1 expression was inhibited after higher doses of both X-rays and C-ions radiation, X-rays induced a more significant increase in PGK1 expression after lower doses radiation (Fig. 3B,C).

Subsequently, we assessed the cell proliferation ability after exposure to different LET radiation. The findings indicated a reduction in cell clone numbers as the irradiation dose increased, particularly notable in the C-ions group (Fig. 3D,E). Specifically, the RBE values for ECA-109 and KYSE-150 cells were determined to be 2.05 and 2.14, respectively. Further analysis revealed that for the X-rays group, the irradiation dose required for cell survival fraction below 50% exceeded 2 Gy, while for C-ions, this threshold was above 1 Gy. In light of this, we selected biologically equivalent doses (4 Gy X-rays and 2 Gy C-ions) for further research in this investigation to ensure biological comparability. Additionally, based on α values from the Linear-Quadratic (LQ) model, ECA-109 cells showed relative resistance to radiation, while KYSE-150 cells were comparatively sensitive (**Supplementary Fig. 2**).

Then, we knocked down and overexpressed PGK1 in two ESCC cells, with the knockdown and overexpression efficiency were confirmed via qRT-PCR (**Supplementary Fig. 1B,C**) and Western blotting (Fig. 3F,G). A plate colony formation assay revealed that both PGK1 knockdown and IR inhibited the proliferation of ESCC cells ($p < 0.01$). Compared to the use of either modality alone, the combination of PGK1 knockdown and IR had significantly stronger antiproliferative effects ($p < 0.01$) (Fig. 4A,C). Overexpression of PGK1 resulted in an enhanced proliferation rate and attenuated the inhibitory impact of IR on cell proliferation ($p < 0.01$) (Fig. 4B,D). These were validated by the CCK8 assay (Fig. 4E,F) and EdU assay (Fig. 4G,H) ($p < 0.05$). Therefore, overexpressing PGK1 can promote ESCC cells growth, whereas knocking down PGK1 enhance the antiproliferative effects induced by IR.

3.3 PGK1 Impacts the Regulation of IR Concerning the ESCC Cells Apoptosis

The flow cytometry results disclosed that the apoptosis level in the combination treatment group was notably higher than that in the single treatment groups ($p < 0.05$) (Fig. 5A). However, overexpression of PGK1 reduced IR-induced apoptosis ($p < 0.01$) (Fig. 5B). These findings display that PGK1 inhibition synergistically induce cell apop-

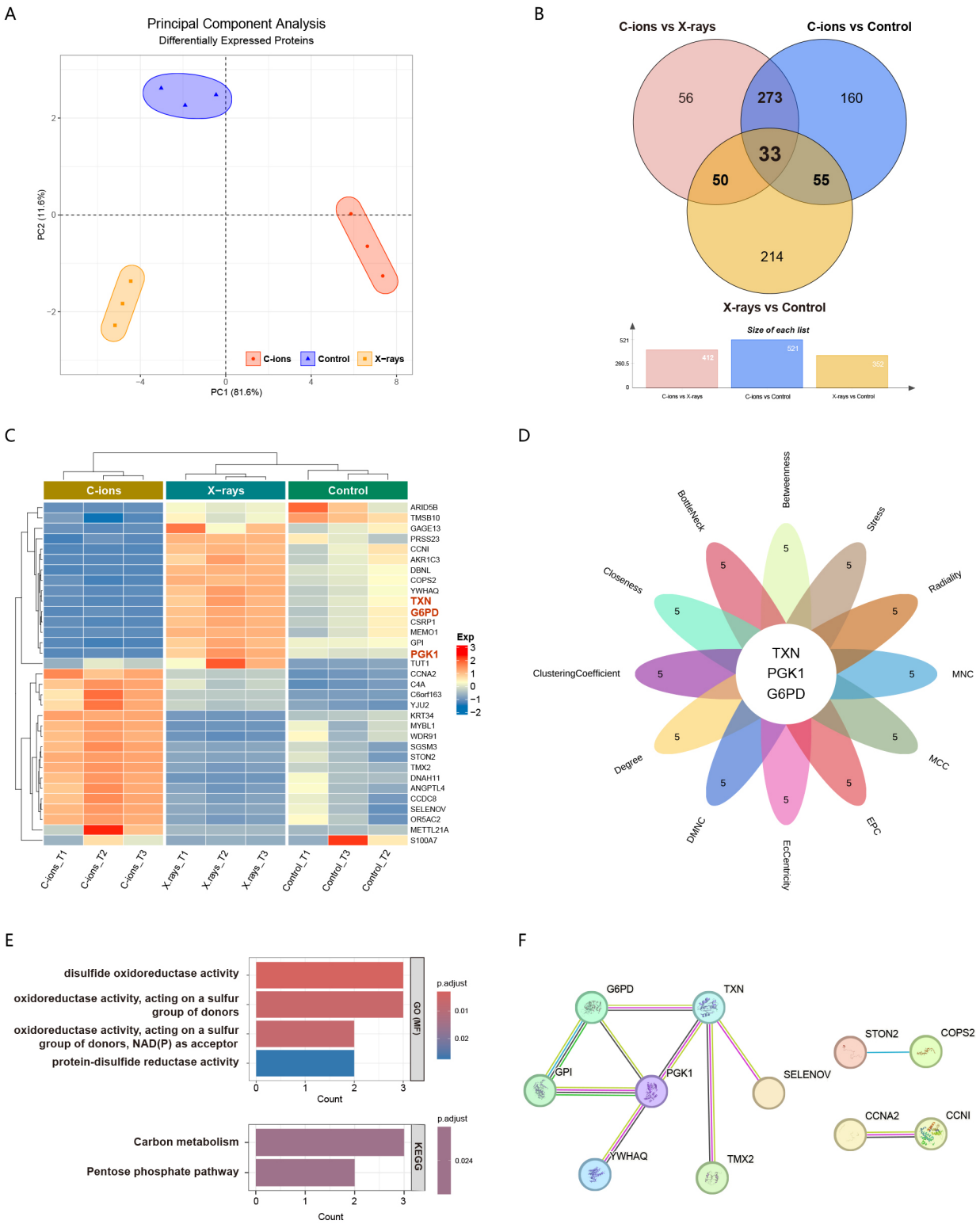

Fig. 1. Screening of the key proteins. (A) PCA of all identified proteins. (B) The Venn diagram shows the overlapped DEPs. (C) A heatmap shows the expression levels of overlapped DEPs in each group of samples, with the proteins highlighted in red are the candidate hub proteins subsequently screened. (D) Venn diagram shows the shared proteins of the top 5 hub proteins of cytoHubba's twelve algorithms. (E) The bar chart visualizes the GO and KEGG enrichment outcomes of overlapping DEPs. (F) The PPI network map generated by the STRING online website shows the relationship between overlapping DEPs interactions. PCA, principal component analysis; DEPs, differentially expressed proteins; GO, gene ontology; KEGG, kyoto encyclopedia of genes and genomes; PGK1, phosphoglycerate kinase 1; TXN, thioredoxin; G6PD, glucose-6-phosphate dehydrogenase.

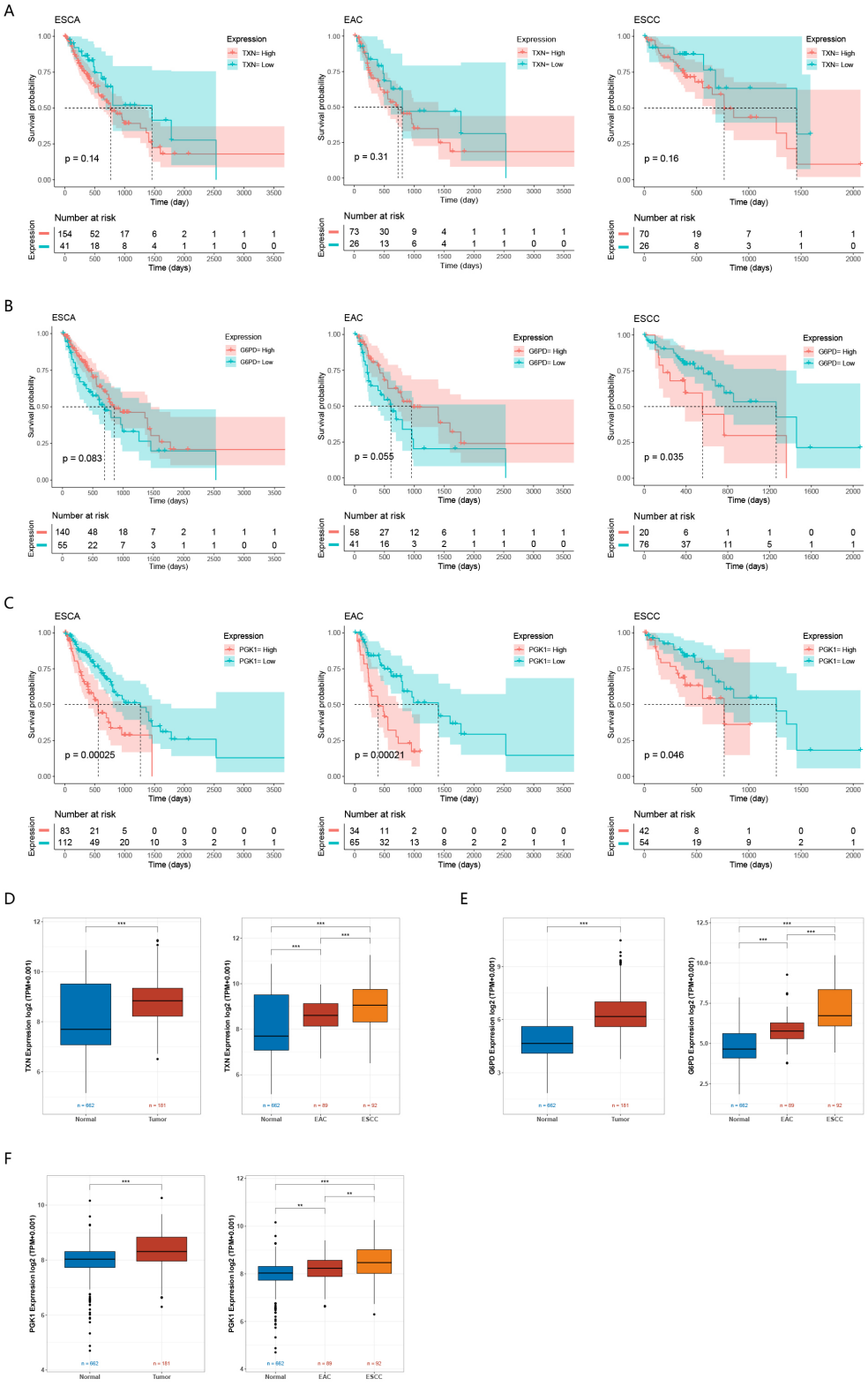

Fig. 2. Kaplan-Meier survival analysis and mRNA expression of candidate genes. Kaplan-Meier survival analysis showing the correlation between *TXN* (A), *G6PD* (B), and *PGK1* (C) mRNA expression and OS of ESCA, EAC, and ESCC patients in TCGA cohort. The mRNA expression levels of *TXN* (D), *G6PD* (E), and *PGK1* (F) in normal esophageal tissues, as well as in ESCA tissues, EAC tissues, and ESCC tissues. EAC, esophageal adenocarcinoma; ESCA, esophageal carcinoma; ESCC, esophageal squamous cell carcinoma. $^{**}p < 0.01$; $^{***}p < 0.001$.

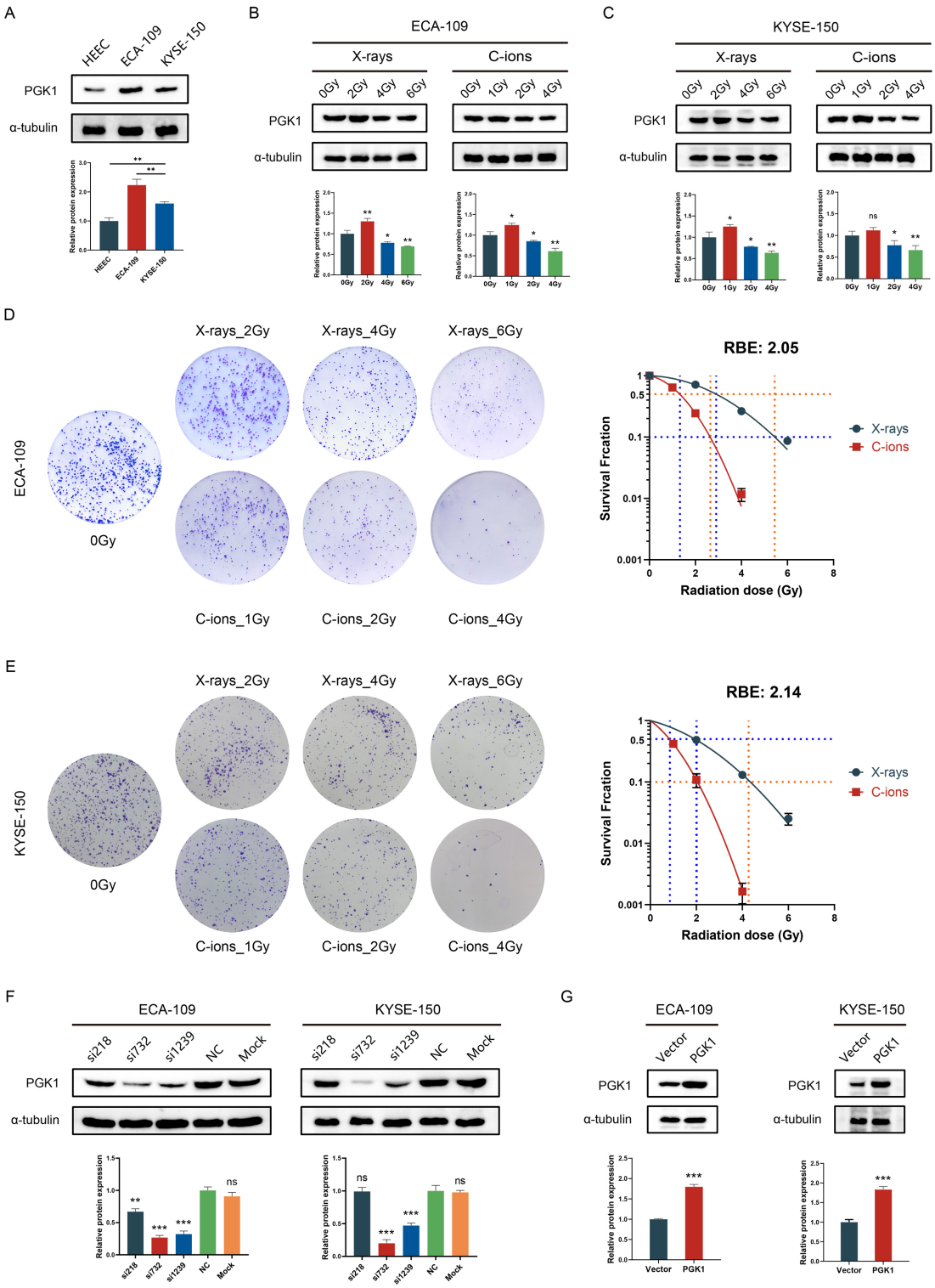

Fig. 3. Analysis of PGK1 protein expression across various cell lines and the impact of varying doses of X-rays or C-ions on clonal survival and PGK1 protein expression in ESCC cells. Protein levels of PGK1 were analyzed in HEEC, ECA-109, and KYSE-150 cell lines (A). PGK1 protein levels were assessed in ESCC cells after different doses of X-rays (B) and C-ions (C). Cloning images and cell survival curves of ECA-109 (D) and KYSE-150 (E) cells after exposure to X-rays and C-ions. Western blot evaluated the efficiency of PGK1 knockdown (F) and PGK1 overexpression (G) in ESCC cells. C-ions, Carbon ions; RBE, relative biological effectiveness. *$p <$ 0.05; **$p < 0.01$; ***$p < 0.001$; and ns, not significant.

tosis with IR.

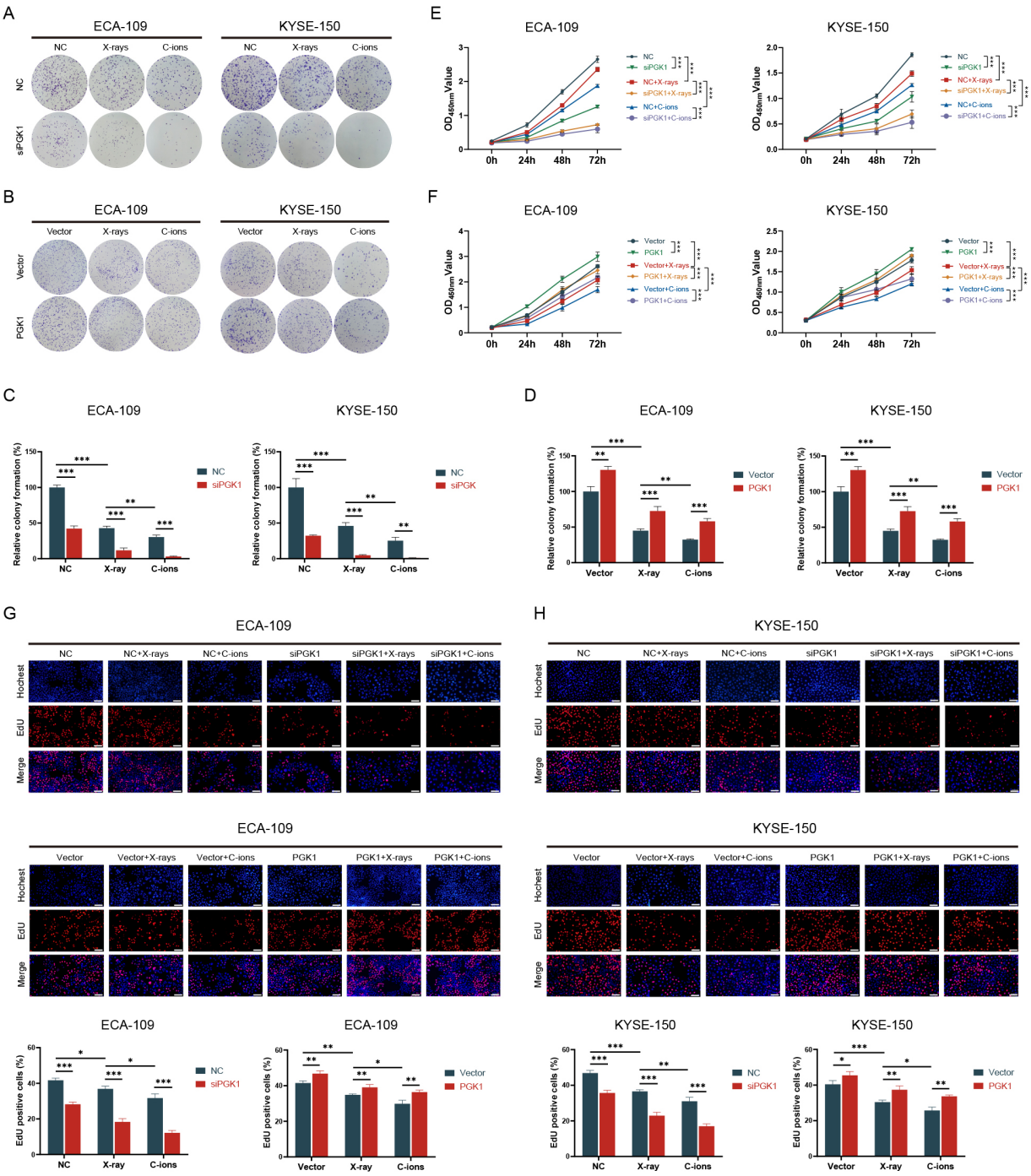

Fig. 4. PGK1 impacts the regulation of IR concerning the ESCC cells proliferation. Plate colony formation assays were conducted to assess clone formation following PGK1 knockdown (A,C) and overexpression (B,D) after IR exposure. Cell viability of ESCC cells with PGK1 knockdown (E) or overexpression (F) was assessed using the CCK8 assay at 24, 48, and 72 h post-IR. An EdU incorporation assay was conducted 48 h post-IR to assess the DNA replication of ECA109 and KYSE150 cells with PGK1 knockdown or overexpression (G,H). CCK8, cell counting kit 8; IR, ionizing radiation; NC, negative control. *$p < 0.05$; **$p < 0.01$; ***$p < 0.001$. Scale bar, 100 μm.

3.4 PGK1 Impacts the Regulation of IR Concerning the Cell Cycle of ESCC Cells

The results showed that regardless of whether IR exposure, PGK1 deficiency elevated the proportion of cells in the G0/G1 phase and reduced those in the G2/M phase ($p <$ 0.05) (Fig. 6A,B). Overexpression of PGK1 significantly elevated the percentage of cells in the G2/M phase while reducing those in the G0/G1 phase ($p < 0.05$) (Fig. 6C,D). In the ECA-109 cell line, both with and without IR, PGK1 knockdown markedly reduced the S-phase cell proportion

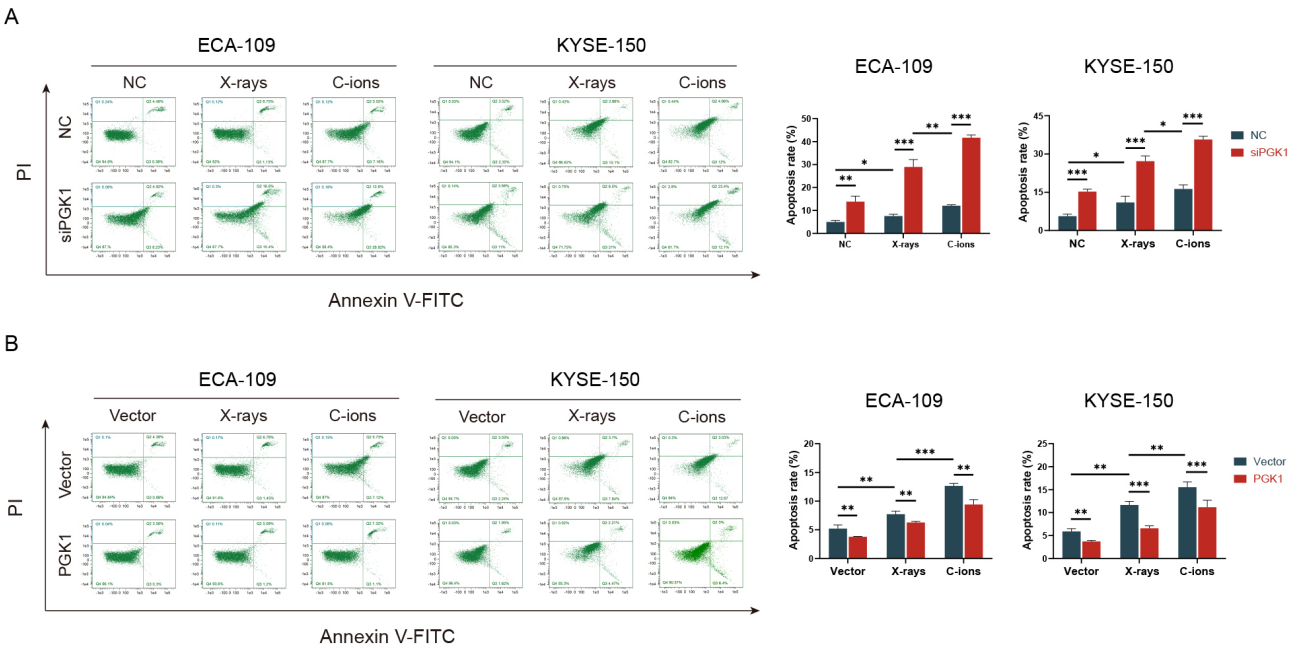

Fig. 5. PGK1 impacts the regulation of IR concerning the ESCC cells apoptosis. The apoptosis levels in ESCC cells with PGK1 knockdown (A) or overexpression (B) after 48 h exposure to IR. *$p < 0.05$; **$p < 0.01$; ***$p < 0.001$.

($p < 0.05$), whereas PGK1 overexpression enhanced it. In KYSE-150 cells, PGK1 knockdown alone diminished S-phase cells, while overexpression notably increased S-phase cell proportion ($p < 0.01$). When exposed to X-rays, both PGK1 knockdown and overexpression resulted in decreased S-phase proportions in KYSE-150 cells ($p < 0.01$). Under C-ions, PGK1 expression status did not significantly influence S-phase distribution (Fig. 6B,D).

3.5 PGK1 Deficiency-Initiated ROS Accumulation and Induced Mitochondrial Dysfunction

IR can cause damage to cells by inducing a substantial increase in ROS levels [12]. Mitochondria serve as the primary source of ROS in mammalian cells. Excessive ROS can lead to mitochondrial dysfunction, which subsequently decreases the MMP and promotes further ROS generation, thereby establishing a detrimental feedback loop that exacerbates cellular damage [13]. We investigated ROS and MMP levels to assess if PGK1 modulates the radiosensitivity of ESCC cells by affecting mitochondrial dysfunction through ROS. The examination of the flow cytometry data indicated that both IR and PGK1 deficiency elevated the fluorescence intensity of DCF staining, with the effect being more significant in the combined group ($p < 0.05$) (Fig. 7A,B). Similarly, both IR and PGK1 deficiency reduced MMP of ESCC cells, and the combined group had a more significant effect ($p < 0.05$) (Fig. 7C,D). Following the use of NAC, an ROS scavenger, the damage to the MMP caused by PGK1 deficiency and IR was restored (Fig. 7E). CCCP, as an uncoupling agent of mitochondrial proton carriers, can destroy the mitochondrial membrane and causing mitochondrial dysfunction. Our findings indicate that overexpressing PGK1 mitigated apoptosis induction ($p < 0.05$) (Fig. 7F) and inhibited proliferation ($p < 0.05$) (Fig. 7G,H) induced by CCCP. Consequently, PGK1 deficiency and IR have synergistic effects on intracellular ROS accumulation and exacerbate mitochondrial damage.

3.6 PGK1 Deficiency Enhances the Radiosensitivity of ESCC Cells via ROS Accumulation

To investigate whether PGK1 modulates the radiosensitivity through ROS, we used ROS scavengers. EdU (Fig. 8A,B) and CCK8 (Fig. 8D) assays showed that NAC partially rescued the impact of PGK1 deficiency and IR on ECA-109 cell proliferation. Similarly, NAC alleviated the apoptosis in ECA-109 cells caused by PGK1 knockdown and IR exposure (Fig. 8C). NAC also had a similar effect on the KYSE-150 cells (**Supplementary Fig. 3**).

3.7 PGK1 Regulates the Akt/mTOR Pathway in ESCC Cells

Inhibition of the Akt/mTOR pathway can effectively augment radiosensitivity [14]. Next, we explored whether PGK1 affects radiosensitivity through the Akt/mTOR pathway. Changes in pathway proteins were detected by Western blotting. Knockdown of PGK1 dramatically curbed the phosphorylation of Akt and mTOR, and intensified the inhibition of this pathway by IR ($p < 0.05$) (Fig. 8E). PGK1 overexpression alleviated the inhibitory effects of IR on the Akt/mTOR pathway ($p < 0.05$) (Fig. 8F). Such findings imply that PGK1 may regulate the radiosensitivity of ESCC cells via the Akt/mTOR pathway.

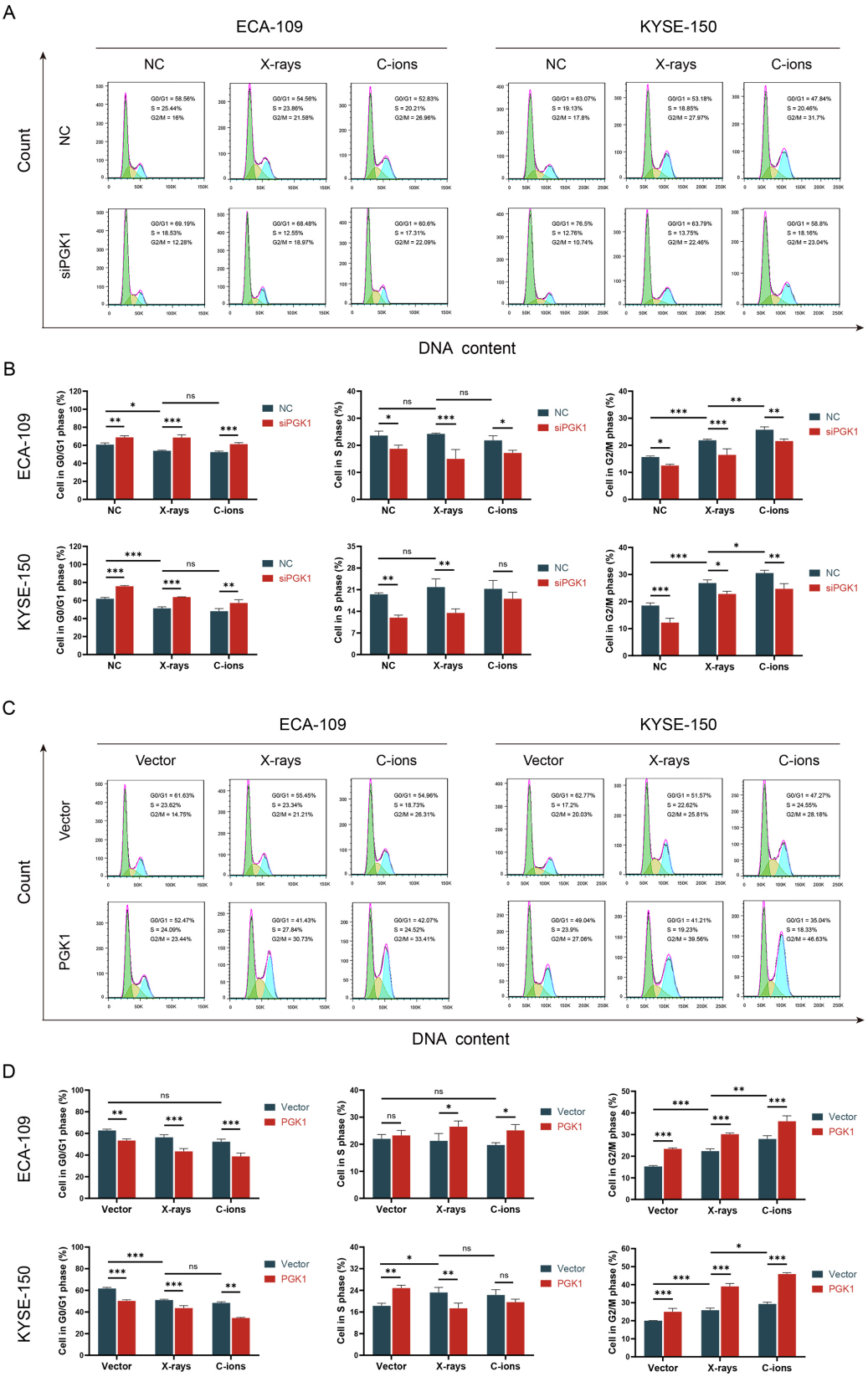

Fig. 6. PGK1 impacts the regulation of IR concerning the cell cycle of ESCC cells. Frequency histograms and statistical analysis charts illustrate the impact of downregulating (A,B) or overexpressing PGK1 (C,D) on cell cycle after 48 h exposure to IR. *$p < 0.05$; **$p < 0.01$; ***$p < 0.001$; and ns, not significant.

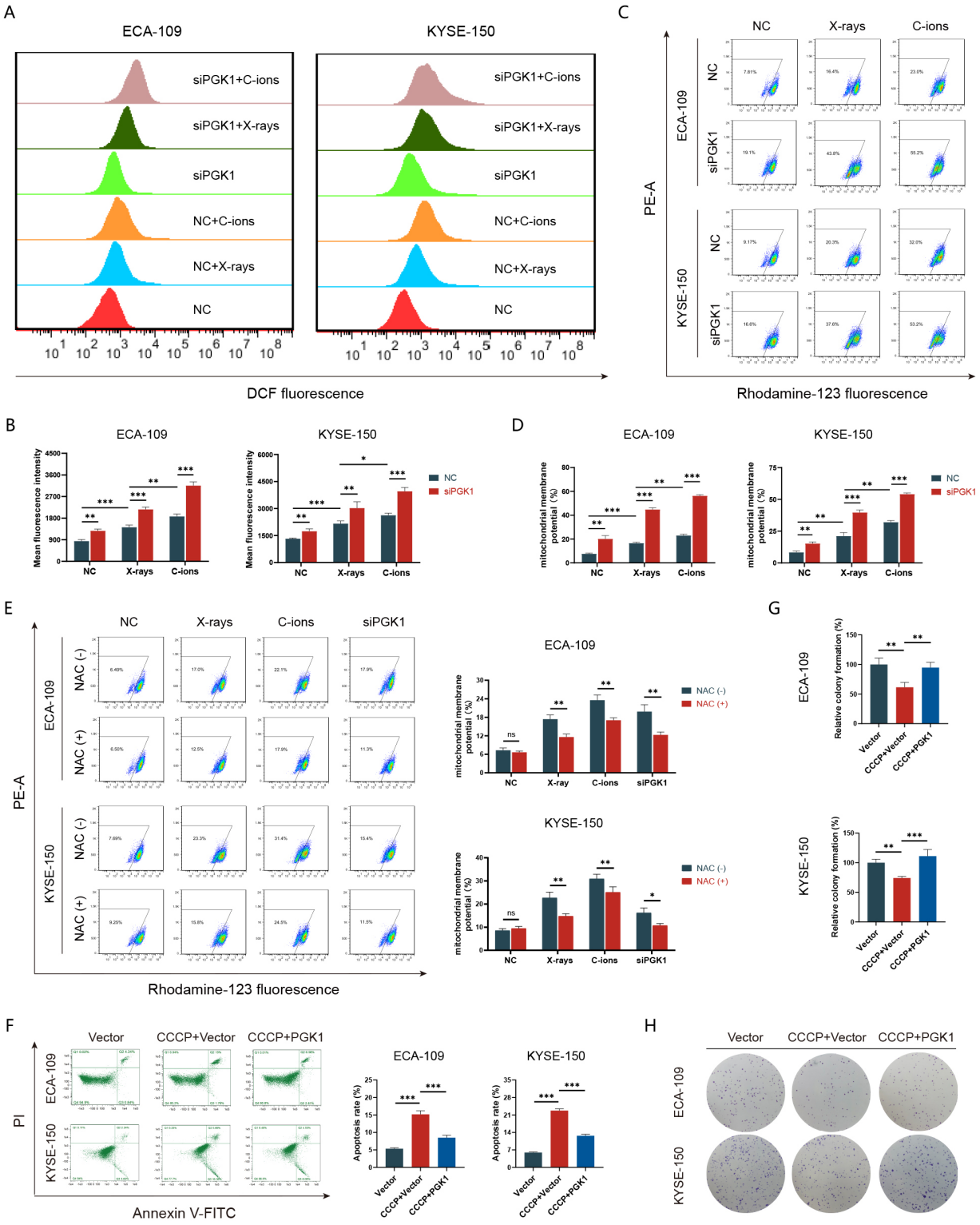

Fig. 7. PGK1 deficiency-initiated ROS accumulation and induced mitochondrial dysfunction. Figures display cytograms and statistical charts illustrating ROS levels in ESCC cells with PGK1 knockdown after 12 h exposure to IR (A,B). Figures display cytograms and statistical analyses of MMP levels of ESCC cells with PGK1 knockdown after 24 h exposure to IR (C,D). The changes in MMP of ESCC cells following PGK1 knockdown or exposure to IR after NAC treatment (E). Apoptotic levels (F) and cloning capacity (G,H) in ESCC cells with PGK1 overexpressed after CCCP treatment. ROS, reactive oxygen species; MMP, mitochondrial membrane potential; NAC, N-acetyl-L-cysteine; CCCP, carbonyl cyanide m-chlorophenylhydrazone. $*p < 0.05$; $**p < 0.01$; $***p < 0.001$; and ns, not significant.

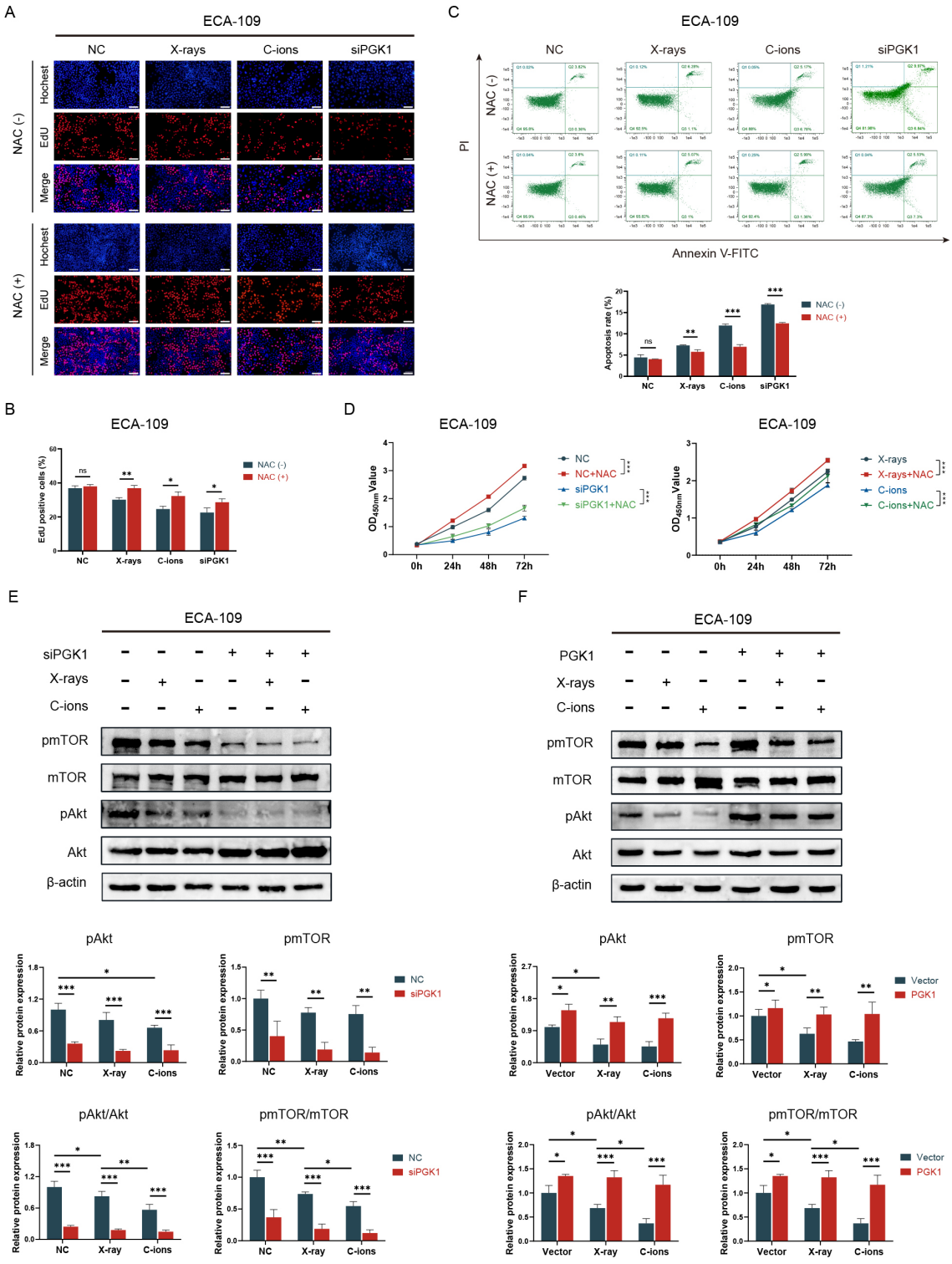

Fig. 8. Following NAC treatment, ECA-109 cell proliferation and apoptosis were assessed with PGK1 knockdown or IR exposure. And the impact of PGK1 on the Akt/mTOR pathway. The DNA replication activity of ECA-109 cells with PGK1 knockdown or IR was detected by EdU incorporation assay following the use of NAC (A,B). The viability of ECA-109 cells with PGK1 knockdown or exposed to IR was determined by CCK8 assay after NAC treatment (D). Apoptosis levels of ECA-109 cells were assessed after PGK1 knockdown or IR with NAC treatment (C). Protein expression levels of Akt, pAkt, mTOR, and pmTOR were analyzed in ECA-109 cells subjected to PGK1 knockdown and IR (E). Protein expression levels of Akt, pAkt, mTOR, and pmTOR were analyzed in ECA-109 cells with PGK1 overexpression and IR (F). *$p < 0.05$; **$p < 0.01$; ***$p < 0.001$; and ns, not significant. Scale bar, 100 μm. Akt/mTOR, protein kinase B/mammalian target of rapamycin.

4. Discussion

Radiotherapy, a critical approach in oncological treatment, while demonstrating significant effectiveness, frequently encounters the challenge of radioresistance. This phenomenon is linked to a higher risk of regional recurrence and distant metastasis after radiation exposure in neoplastic cells, representing a substantial hurdle in the realm of radiotherapy that necessitates urgent resolution [15]. Recent investigations have suggested that PGK1 is crucial in the radiosensitivity regulatory network of tumors, and its inhibition can enhance the radiosensitivity of glioma and colorectal cancer cells [16,17]. Nevertheless, the intricate relationship between PGK1 and ionizing radiation, particularly the specific mechanisms by which it influences radiosensitivity in cancer cells, remains largely unexplored. This research concentrates on ESCC, with the objective of examining the regulatory function of PGK1 in the radiosensitivity of ESCC cells and elucidating its underlying mechanisms.

In comparison to traditional X-ray radiation, CIRT has gained considerable recognition in the field of oncology due to its dual benefits of precise physical dose distribution and distinct biological characteristics [18,19]. A wealth of clinical evidence indicates that CIRT can significantly improve local tumor control and patient survival rates while simultaneously minimizing treatment-related adverse effects and complications [20]. Particularly in the management of radiation-resistant and recurrent tumors, CIRT has demonstrated unique therapeutic benefits, providing renewed hope for these challenging cases [21–23]. Various radiation types and doses may induce differences in gene expression, reflecting the functional regulatory mechanisms present in diverse radiation contexts [24]. In this investigation, mass spectrometry analysis revealed notable differences in PGK1 expression in ESCC cells following exposure to X-rays and C-ions. To precisely evaluate this difference and assess the practical comparative significance of biological effects, we calculated the relative RBE values of C-ions for two ESCC cell lines. Additionally, we analyzed PGK1 protein expression in ESCC cells following X-ray and carbon ion radiation at varying doses. Our results indicated that, at equivalent RBE doses, the patterns of PGK1 protein expression influenced by X-rays and C-ions were analogous: under low-dose radiation, PGK1 protein expression was upregulated, which may suggest a cellular protective response against radiation-induced damage, consequently promoting tumor cell survival and reducing the effectiveness of radiotherapy; In contrast, at high-dose radiation, PGK1 protein expression was downregulated, likely due to radiation directly activating apoptotic and necrotic pathways instead of stimulating protective mechanisms. Furthermore, under low-dose radiation, the upregulation of PGK1 by C-ions was less pronounced than that induced by X-rays, possibly due to the more significant direct damage caused by C-ions, which restricts the activation of radiation resistance pathways. This further highlights the intricate nature of tumor cell responses to various radiation modalities.

PGK1 drives proliferation, angiogenesis, migration, invasion and epithelial-mesenchymal transition (EMT) of cancer cells by regulating a variety of biological processes [8,25]. An in-depth multi-omics study of ESCC patients identified PGK1 as a potential therapeutic target in ESCC progression [26]. Xu *et al*. [27] illustrated that NRSN2-AS1, a long non-coding RNA, can interact with PGK1 to enhance its protein expression, which in turn promotes ESCC cell proliferation, migration, invasion, and EMT. Our research examined the function of PGK1 in ESCC cells through both knockdown and overexpression experiments, revealing that PGK1 facilitates the proliferation of ESCC cells while inhibiting apoptosis. Conversely, the suppression of PGK1 yielded opposing effects. These findings suggest that PGK1 exerts a tumor-promoting influence in ESCC cells.

To clarify PGK1's role in ESCC cell radiation response, we exposed ESCC cells with PGK1 knockdown or overexpression to X-ray and C-ion irradiation. The findings revealed that overexpressing PGK1 attenuated the inhibitory effect of IR on cell proliferation and the promotive effect on apoptosis, while knockdown of PGK1 enhanced these effects. This indicates a notable association between PGK1 and the radiosensitivity of cancer cells. This is consistent with previous research findings. Targeted silencing of PGK1 via shRNA technology has been shown to markedly increase the radiosensitivity of glioblastoma [28,29]. These observations indicate that PGK1 is crucial in developing radioresistance in tumor cells and is a potential target for altering cancer cell radiosensitivity.

Next, we probed into the possible mechanisms through which PGK1 affects the efficacy of IR. While inducing DNA damage to kill tumor cells, IR also activates the DNA damage repair network to promote DNA repair [30,31]. A key manifestation of this response is the induction of G2/M phase arrest, which provides sufficient time for the repair of DNA lesion [30]. A previous study has indicated that a PGK1 inhibitor (Z57346765) can impair the DNA damage repair capacity, resulting in cell cycle arrest in the G1/S phase and consequently inhibiting the growth of clear cell renal carcinoma cells [32]. The results of our study corroborate their findings. This significant discovery implies that PGK1 might be involved in IR-induced DNA damage repair through its participation in cell cycle regulation.

The augmented ability to scavenge ROS constitutes one of the several factors contributing to the emergence of radioresistance in ESCC [33]. ROS are pivotal in controlling cellular processes such as migration, differentiation, proliferation, and apoptosis. Specifically, an overabundance of ROS can inflict cellular damage and trigger apoptosis, while a moderate increase in ROS may facilitate malignant transformation and tumor progression [34]. Cancer cells meticulously modulate intracellular ROS through

diverse mechanisms to avert death induced by excessive ROS accumulation. Mitochondria serve as both the principal source of ROS generation and the primary target of ROS-induced damage, which can ultimately culminate in cell death [34]. IR kills cancer cells by increasing intracellular ROS in a dose-dependent manner [12]. PGK1 phosphorylates pyruvate dehydrogenase kinase 1 (PDHK1), enhancing glycolytic flux by preventing pyruvate from entering the tricarboxylic acid cycle. This cascade of events suppresses mitochondrial respiration, diminishes ROS production, and consequently fosters the proliferation and advancement of tumor cells while effectively preventing cell death due to excessive ROS [35]. Targeted therapies aimed at inhibiting PGK1 can elevate ROS levels via this pathway, thereby not only curtailing the proliferation and EMT of glioma cells but also promoting glioma cell apoptosis [36]. Accordingly, we speculate that the inhibition of PGK1 may enhance radiosensitivity through an increase in ROS. To test this hypothesis, we utilized flow cytometry to measure the fluorescence intensity of DCF as an indicator for ROS levels. The results demonstrated that the inhibition of PGK1 increased ROS production and exacerbated the reduction of MMP in ESCC cells exposed to IR. The application of NAC to scavenge ROS resulted in a partial restoration of MMP damage compromised by PGK1 downregulation, as well as a mitigation of IR-induced MMP damage. Additionally, the overexpression of PGK1 diminished apoptosis induced by CCCP and lessened CCCP's inhibitory impact on cell proliferation. In summary, the findings strongly suggest that PGK1 influences the radiosensitivity of ESCC cells by regulating mitochondrial ROS production.

PGK1-mediated carcinogenesis is also associated with the AKT/mTOR signaling pathway. Studies established that PGK1-driven activation of the AKT/mTOR pathway enhances tumor growth, metastasis, and EMT, as well as contributing to cancer recurrence [37,38]. Suppression of the PI3K/Akt/mTOR pathway has been shown to augment radiosensitivity [14]. Throughout the evolution and advancement of cancer cells, ROS interact with Akt to modulate their malignant characteristics. Akt activation can stimulate ROS production, whereas elevated ROS levels can lead to Akt protein inactivation, ultimately triggering cancer cell apoptosis [39]. This study indicated that PGK1 deficiency inhibits the Akt and mTOR phosphorylation, indicating PGK1's potential role in modulating cancer cell radiosensitivity via this pathway.

It is noteworthy that, despite using the RBE dose for comparison in this study, it was observed that 2 Gy of C-ions demonstrated a more potent cytotoxic effect compared to 4 Gy of X-rays. This may be related to the quantity and distribution of ROS induced by C-ions. Research indicates that C-ions are capable of producing a greater amount of ROS, resulting in more extensive mitochondrial impairment [18]. In addition, the radicals induced by C-ions are clustered and concentrated in the trajectories of the particles, while the ROS induced by X-rays show a diffuse distribution. Such clustered radicals induced by C-ions cause more severe and complex damage to cells, while the extremely low production of radicals outside the tracks cannot trigger the cellular defense mechanism [40].

Of course, there are some limitations to this study. First, our experiment lacks *in vivo* validation. Secondly, further investigation is required to elucidate the detailed molecular process mediating the engagement of PGK1 with the Akt/mTOR signaling pathway. In addition, the radiosensitization effect of PGK1 inhibitors and their potential application in clinical radiotherapy need to be further evaluated. Nevertheless, this study reveals a novel function of PGK1 in modulating the radiosensitivity of ESCC, providing an important basis for its clinical translational potential as a radiotherapy sensitization target.

5. Conclusions

PGK1 is overexpressed in ESCC cells, promoting cancer cell survival, proliferation, and radioresistance by decreasing intracellular ROS and activating the Akt/mTOR signaling pathway. This research offers novel insights into the mechanisms that affect ESCC radiosensitivity and underscores PGK1's potential as a therapeutic target for ESCC.

Availability of Data and Materials

The datasets used and/or analyzed during the current study are available from the corresponding author on reasonable request.

Author Contributions

JRC: conceptualization, methodology, software and writing - original draft. HTL: conceptualization, validation, funding acquisition and project management. XW: visualization and investigation. MD: investigation and formal analysis. DDW: formal analysis. YHO: visualization, YHW: data curation. SLS: data curation and resources. ZQL: formal analysis. ZY: data curation. QLG: methodology, project administration and supervision. QNZ: conceptualization, project administration, funding acquisition and writing - review & editing. All authors contributed to editorial changes in the manuscript. All authors read and approved the final manuscript. All authors have participated sufficiently in the work and agreed to be accountable for all aspects of the work.

Ethics Approval and Consent to Participate

Not applicable.

Acknowledgment

All authors sincerely thank Professor Wang Xiaohu for his guidance in this study.

Funding

The study was supported by the Central guidance local science and technology development program (Grant No. 24ZYQA029), the National Key Research and Development Program of China (No. 2022YFC2401500), Science and Technology Project of Lanzhou City (Grant No. 2023-1-9), Gansu Province Project of Science and Technologies (Grant No. 20JR10RA680, 22CX8JA149), Gansu Provincial Natural Science Foundation (No.25JRRA265) and the Lanzhou heavy Ion Accelerator High-end user Project (Grant No. HIR20GY007).

Conflict of Interest

The authors declare that they have no competing interests.

Supplementary Material

Supplementary material associated with this article can be found, in the online version, at https://doi.org/10.31083/FBL36430.

References

[1] He S, Xia C, Li H, Cao M, Yang F, Yan X, *et al*. Cancer profiles in China and comparisons with the USA: a comprehensive analysis in the incidence, mortality, survival, staging, and attribution to risk factors. Science China. Life Sciences. 2024; 67: 122–131. https://doi.org/10.1007/s11427-023-2423-1.

[2] Santucci C, Mignozzi S, Malvezzi M, Collatuzzo G, Levi F, La Vecchia C, *et al*. Global trends in esophageal cancer mortality with predictions to 2025, and in incidence by histotype. Cancer Epidemiology. 2023; 87: 102486. https://doi.org/10.1016/j.canep.2023.102486.

[3] Zhu H, Ma X, Ye T, Wang H, Wang Z, Liu Q, *et al*. Esophageal cancer in China: Practice and research in the new era. International Journal of Cancer. 2023; 152: 1741–1751. https://doi.org/10.1002/ijc.34301.

[4] Wu X, Hu X, Chen J, He L. A re-irradiation dose of 55-60 Gy improves the survival rate of patients with local recurrent esophageal squamous cell carcinoma after radiotherapy. Radiation Oncology (London, England). 2021; 16: 100. https://doi.org/10.1186/s13014-021-01828-z.

[5] Xu Y, Dong B, Zhu W, Li J, Huang R, Sun Z, *et al*. A Phase III Multicenter Randomized Clinical Trial of 60 Gy versus 50 Gy Radiation Dose in Concurrent Chemoradiotherapy for Inoperable Esophageal Squamous Cell Carcinoma. Clinical Cancer Research: an Official Journal of the American Association for Cancer Research. 2022; 28: 1792–1799. https://doi.org/10.1158/1078-0432.CCR-21-3843.

[6] Shao F, Yang X, Wang W, Wang J, Guo W, Feng X, *et al*. Associations of PGK1 promoter hypomethylation and PGK1-mediated PDHK1 phosphorylation with cancer stage and prognosis: a TCGA pan-cancer analysis. Cancer Communications (London, England). 2019; 39: 54. https://doi.org/10.1186/s40880-019-0401-9.

[7] Fu Q, Yu Z. Phosphoglycerate kinase 1 (PGK1) in cancer: A promising target for diagnosis and therapy. Life Sciences. 2020; 256: 117863. https://doi.org/10.1016/j.lfs.2020.117863.

[8] Zhang K, Sun L, Kang Y. Regulation of phosphoglycerate kinase 1 and its critical role in cancer. Cell Communication and Signaling: CCS. 2023; 21: 240. https://doi.org/10.1186/s12964-023-01256-4.

[9] Isozaki T, Ishikawa H, Yamada S, Nabeya Y, Minashi K, Murakami K, *et al*. Outcomes of definitive carbon-ion radiotherapy for cT1bN0M0 esophageal squamous cell carcinoma. Esophagus: Official Journal of the Japan Esophageal Society. 2024; 21: 523–529. https://doi.org/10.1007/s10388-024-01067-7.

[10] Ma N, Ming X, Chen J, Wu KL, Lu J, Jiang G, *et al*. Dosimetric rationale and preliminary experience in proton plus carbon-ion radiotherapy for esophageal carcinoma: a retrospective analysis. Radiation Oncology (London, England). 2023; 18: 195. https://doi.org/10.1186/s13014-023-02371-9.

[11] Luo H, Yang Z, Zhang Q, Li T, Liu R, Feng S, *et al*. LIF Inhibits Proliferation of Esophageal Squamous Carcinoma Cells by Radiation Mediated Through JAK-STAT Signaling Pathway. Journal of Cancer. 2023; 14: 532–543. https://doi.org/10.7150/jca.81222.

[12] Nakamura H, Takada K. Reactive oxygen species in cancer: Current findings and future directions. Cancer Science. 2021; 112: 3945–3952. https://doi.org/10.1111/cas.15068.

[13] Kam WWY, Banati RB. Effects of ionizing radiation on mitochondria. Free Radical Biology & Medicine. 2013; 65: 607–619. https://doi.org/10.1016/j.freeradbiomed.2013.07.024.

[14] Wanigasooriya K, Tyler R, Barros-Silva JD, Sinha Y, Ismail T, Beggs AD. Radiosensitising Cancer Using Phosphatidylinositol-3-Kinase (PI3K), Protein Kinase B (AKT) or Mammalian Target of Rapamycin (mTOR) Inhibitors. Cancers. 2020; 12: 1278. https://doi.org/10.3390/cancers12051278.

[15] Larionova I, Rakina M, Ivanyuk E, Trushchuk Y, Chernyshova A, Denisov E. Radiotherapy resistance: identifying universal biomarkers for various human cancers. Journal of Cancer Research and Clinical Oncology. 2022; 148: 1015–1031. https://doi.org/10.1007/s00432-022-03923-4.

[16] Islam Khan MZ, Tam SY, Azam Z, Law HKW. Proteomic profiling of metabolic proteins as potential biomarkers of radioresponsiveness for colorectal cancer. Journal of Proteomics. 2022; 262: 104600. https://doi.org/10.1016/j.jprot.2022.104600.

[17] Wang Z, Tang XL, Zhao MJ, Zhang YD, Xiao Y, Liu YY, *et al*. Biomimetic hypoxia-triggered RNAi nanomedicine for synergistically mediating chemo/radiotherapy of glioblastoma. Journal of Nanobiotechnology. 2023; 21: 210. https://doi.org/10.1186/s12951-023-01960-w.

[18] Averbeck D, Rodriguez-Lafrasse C. Role of Mitochondria in Radiation Responses: Epigenetic, Metabolic, and Signaling Impacts. International Journal of Molecular Sciences. 2021; 22: 11047. https://doi.org/10.3390/ijms222011047.

[19] Tinganelli W, Durante M. Carbon Ion Radiobiology. Cancers. 2020; 12: 3022. https://doi.org/10.3390/cancers12103022.

[20] Yun JE, Kim S, Park KY, Lee W. Effectiveness and Safety of Carbon Ion Radiotherapy in Solid Tumors: A Systematic Review and Meta-Analysis. Yonsei Medical Journal. 2024; 65: 332–340. https://doi.org/10.3349/ymj.2023.0439.

[21] Yamada S, Takiyama H, Isozaki Y, Shinoto M, Ebner DK, Koto M, *et al*. Carbon Ion Radiotherapy for Locally Recurrent Rectal Cancer of Patients with Prior Pelvic Irradiation. Annals of Surgical Oncology. 2022; 29: 99–106. https://doi.org/10.1245/s10434-021-10876-4.

[22] Lu VM, O'Connor KP, Mahajan A, Carlson ML, Van Gompel JJ. Carbon ion radiotherapy for skull base chordomas and chondrosarcomas: a systematic review and meta-analysis of local control, survival, and toxicity outcomes. Journal of Neuro-oncology. 2020; 147: 503–513. https://doi.org/10.1007/s11060-020-03464-1.

[23] Liermann J, Ben-Josef E, Syed M, Debus J, Herfarth K, Naumann P. Carbon ion radiotherapy as definitive treatment in locally recurrent pancreatic cancer. Strahlentherapie Und Onkologie. 2022; 198: 378–387. https://doi.org/10.1007/s00066-021-01827-9.

[24] Zhang J, Si J, Gan L, Zhou R, Guo M, Zhang H. Harnessing the targeting potential of differential radiobiological effects of

photon versus particle radiation for cancer treatment. Journal of Cellular Physiology. 2021; 236: 1695–1711. https://doi.org/10.1002/jcp.29960.

[25] Chen J, Wu X, Luo H, Wang D, Dong M, Wang Y, *et al*. Pan-cancer investigation regarding the prognostic predictive and immunological regulation functions of PGK1 and experimental validation in esophageal squamous cell carcinoma. Functional & Integrative Genomics. 2025; 25: 54. https://doi.org/10.1007/s10142-025-01555-8.

[26] Li L, Jiang D, Zhang Q, Liu H, Xu F, Guo C, *et al*. Integrative proteogenomic characterization of early esophageal cancer. Nature Communications. 2023; 14: 1666. https://doi.org/10.1038/s41467-023-37440-w.

[27] Xu T, Yan Z, Lu J, Chen L, Li X, Li Y, *et al*. Long non-coding RNA NRSN2-AS1, transcribed by SOX2, promotes progression of esophageal squamous cell carcinoma by regulating the ubiquitin-degradation of PGK1. Clinical & Experimental Metastasis. 2022; 39: 757–769. https://doi.org/10.1007/s10585-022-10174-7.

[28] Cheng YJ, Ding H, Du HQ, Yan H, Zhao JB, Zhang WB, *et al*. Downregulation of phosphoglycerate kinase 1 by shRNA sensitizes U251 xenografts to radiotherapy. Oncology Reports. 2014; 32: 1513–1520. https://doi.org/10.3892/or.2014.3353.

[29] Ding H, Cheng YJ, Yan H, Zhang R, Zhao JB, Qian CF, *et al*. Phosphoglycerate kinase 1 promotes radioresistance in U251 human glioma cells. Oncology Reports. 2014; 31: 894–900. https://doi.org/10.3892/or.2013.2874.

[30] Larsen BD, Benada J, Yung PYK, Bell RAV, Pappas G, Urban V, *et al*. Cancer cells use self-inflicted DNA breaks to evade growth limits imposed by genotoxic stress. Science (New York, N.Y.). 2022; 376: 476–483. https://doi.org/10.1126/science.abi6378.

[31] Ray U, Raghavan SC. Inhibitors of DNA double-strand break repair at the crossroads of cancer therapy and genome editing. Biochemical Pharmacology. 2020; 182: 114195. https://doi.org/10.1016/j.bcp.2020.114195.

[32] He Y, Luo Y, Huang L, Zhang D, Hou H, Liang Y, *et al*. Novel inhibitors targeting the PGK1 metabolic enzyme in glycolysis exhibit effective antitumor activity against kidney renal clear cell carcinoma in vitro and in vivo. European Journal of Medicinal Chemistry. 2024; 267: 116209. https://doi.org/10.1016/j.ejmech.2024.116209.

[33] An L, Li M, Jia Q. Mechanisms of radiotherapy resistance and radiosensitization strategies for esophageal squamous cell carcinoma. Molecular Cancer. 2023; 22: 140. https://doi.org/10.1186/s12943-023-01839-2.

[34] Moloney JN, Cotter TG. ROS signalling in the biology of cancer. Seminars in Cell & Developmental Biology. 2018; 80: 50–64. https://doi.org/10.1016/j.semcdb.2017.05.023.

[35] Li X, Jiang Y, Meisenhelder J, Yang W, Hawke DH, Zheng Y, *et al*. Mitochondria-Translocated PGK1 Functions as a Protein Kinase to Coordinate Glycolysis and the TCA Cycle in Tumorigenesis. Molecular Cell. 2016; 61: 705–719. https://doi.org/10.1016/j.molcel.2016.02.009.

[36] Wang WL, Jiang ZR, Hu C, Chen C, Hu ZQ, Wang AL, *et al*. Pharmacologically inhibiting phosphoglycerate kinase 1 for glioma with NG52. Acta Pharmacologica Sinica. 2021; 42: 633–640. https://doi.org/10.1038/s41401-020-0465-8.

[37] Jiang Q, Wang Z, Qi Q, Li J, Xin Y, Qiu J. lncRNA SNHG26 promoted the growth, metastasis, and cisplatin resistance of tongue squamous cell carcinoma through PGK1/Akt/mTOR signal pathway. Molecular Therapy Oncolytics. 2021; 24: 355–370. https://doi.org/10.1016/j.omto.2021.12.021.

[38] Luo H, Li Q, Wang RT, Zhang L, Zhang W, Deng MS, *et al*. Downregulation of pro-surfactant protein B contributes to the recurrence of early-stage non-small cell lung cancer by activating PGK1-mediated Akt signaling. Experimental Hematology & Oncology. 2023; 12: 94. https://doi.org/10.1186/s40164-023-00455-6.

[39] Hua H, Zhang H, Chen J, Wang J, Liu J, Jiang Y. Targeting Akt in cancer for precision therapy. Journal of Hematology & Oncology. 2021; 14: 128. https://doi.org/10.1186/s13045-021-01137-8.

[40] Wozny AS, Rodriguez-Lafrasse C. The 'stealth-bomber' paradigm for deciphering the tumour response to carbon-ion irradiation. British Journal of Cancer. 2023; 128: 1429–1438. https://doi.org/10.1038/s41416-022-02117-6.